RAPID COMMUNICATIONS

PHYSICAL REVIEW E VOLUME 47, NUMBER 5 MAY 1993

Scattering and wavelength transduction of diffuse photon density waves

D. A. Boas and M. A. O'Leary
Department of Physics and Department of Biochemistry and Biophysics, University of Pennsylvania, Philadelphia, Pennsylvania 19104-6396

B. Chance
Department of Biochemistry and Biophysics, University of Pennsylvania, Philadelphia, Pennsylvania 19104-6396

A. G. Yodh
Department of Physics, University of Pennsylvania, Philadelphia, Pennsylvania 19104-6396
(Received 22 December 1992)

Experiments are performed that illustrate the scattering and reradiation of damped traveling waves of light energy density from objects within otherwise homogeneous turbid media. We demonstrate that simple diffractive and refractive models can be used to understand the scattering of these waves by absorptive and dispersive spheres. Furthermore, using a fluorescent dye we can reestablish the origin of the diffuse photon density waves, by converting from one optical and diffusive wavelength to another while maintaining phase coherence. The possibilities for precise medical imaging are presented.

PACS number(s): 42.25.Gy, 42.62.Be, 41.20.Jb, 42.25.Md

Diffuse photon density waves are just beginning to receive attention as a result of intrinsic interest in their phenomenology and because of their propensity to provide information about the dense random media through which they move. Briefly, diffuse photon density waves are scalar, overdamped, traveling waves of light energy density. They will propagate through any medium in which the transport of light energy density, $U(\mathbf{r},t)$, is governed by the diffusion equation [1], $\partial U/\partial t = D\nabla^2 U$, where D is the light diffusion constant in the medium. Examples of such media for visible light include dense colloidal suspensions of micrometer-size spheres, human tissue, paints, foams, and Intralipid. The traveling waves are produced by introducing amplitude modulated light, with source modulation frequency ω, into the optically turbid medium [2–6].

In essence, the introduction of amplitude-modulated light into the turbid medium produces a *macroscopic ripple of brightness* that is *microscopically* composed of individual photons undergoing random walks. The macroscopic disturbance obeys a Helmholtz equation, and therefore has many properties that we normally associate with conventional electromagnetic radiation. In a recent paper, for example, we have demonstrated the refraction of these waves [5]. Other experiments that have been accomplished recently exhibit aspects of simple diffraction [4] and interference [3,7] using these waves.

In this paper we investigate the scattering and reradiation of diffuse photon density waves by obstacles located within otherwise turbid homogeneous media. The reradiation experiments introduce a new and potentially useful physical phenomenon that is brought about through the interaction of these waves with fluorescent scattering inhomogeneities, and the scattering experiments demonstrate the utility of two conceptually simple diffractive and refractive models for wave-front distortion. The measurements span two approaches to the detection of localized inhomogeneities within optically dense media. At the conclusion of this paper we will comment briefly on the biomedical potential of the two approaches.

In the first set of experiments we have observed the conversion or transduction of a diffuse photon density wave from one *optical and diffusive* wavelength to another. This was accomplished by illuminating an obstacle filled with absorbing dye by a diffuse photon density wave. The dye was chosen to absorb radiation at the source wavelength, and very soon thereafter to *reradiate* photons at a red-shifted energy. Because the dye had a lifetime of less than 1 nsec compared to the 5-nsec period of the source, the reradiated energy was also in the form of a diffuse photon density wave that was readily detected at the red-shifted energy. This phenomenon might be described as a type of "fluorescence" of a diffuse photon density wave. In the process, the inhomogeneity is converted into a *source* of diffuse photon density waves. Localization of the obstacle can be accomplished by determination of the source center from the reradiated wave fronts.

In the second set of experiments we have measured the wave-front distortions that arise when these waves are scattered by purely absorptive or dispersive homogeneous spheres. In general, one would expect both refractive and diffractive processes to affect the scattered wave fronts. Unfortunately, our intuition from conventional optics is of limited applicability, since we must work in the near field. We have found that measurements of wave-front distortions from purely absorbing spheres are well described by a simple diffraction model whereby the diffuse photon density wave is scattered by an absorbing disk of the same diameter. The pure dispersive case is more complex. A ray optic model works well for scatterers characterized by a larger light diffusion constant relative to that of the surrounding turbid medium, but a diffractive model is required in the other limit.

Our scheme for the generation, propagation, and detection of diffuse photon density waves has been described [5]. The diffuse medium is Intralipid solution [8], in which an amplitude-modulated (200-MHz 1-mW diode laser operating at either 780 nm or 816 nm is inserted. In a homogeneous medium, the oscillating part of the light energy density radiated by the source has the form $U(\mathbf{r},t) = (A/Dr)\exp[-k(\cos\phi)r]\exp\{i[k(\sin\phi)r-\omega t]\}$ where A is a constant and $k=(\omega/D)^{1/2}$, and for a medium characterized by absorption length l_a and optical index of refraction n, $\tan 2\phi=(\omega l_a)(n/c)$. Absorptive corrections to k and D are relatively small for the samples we consider.

Light is delivered into the sample through a source fiber and is collected by a movable detector fiber. The oscillating part of the diffuse light energy density is measured by standard phase-sensitive methods. Typically we determine the amplitude and phase of the diffuse photon density wave at the movable detector as a function of its position in the medium. In the present experiments we also introduce spherical obstacles into the medium.

The primary results of our reradiation experiments are shown in Fig. 1. Here the source laser is located at the origin, and a 1.8-cm-diam transparent spherical shell filled with a 0.1% solution of Intralipid is located a distance of 4.5 cm from the source. The surrounding Intralipid has the same concentration, giving a photon diffusion constant $D=6.0\times10^9$ cm^2/sec. A biologically useful dye, indocyanine green [9] was dissolved in the spherical shell at a concentration of 0.41 μg/cm^3. The indocyanine green absorbed light from the incident diffuse photon density wave at 780 nm, and then emitted photons at 830 nm. The absorption and emission characteristics of the indocyanine green are shown in Fig. 1(a). Since the lifetime of the dye is relatively short (<1 nsec), the reradiated radiation was also in the form of a diffuse photon density wave. Using spectral filters we separately measured the incident wave at 780 nm in the presence of the obstacle, and the reradiated wave at 830 nm. The latter measurement can in principle have zero background.

In Fig. 1(b) the constant amplitude contours of the diffuse photon density wave at 780 nm are presented at intervals that decrease by a factor of 0.3 with increasing distance from the source. We see that these contours are reasonably circular and can be extrapolated back to the laser source. The small deviations observed are primarily a result of absorption by the obstacle. A similar contour plot of the phase was also measured, and could also be extrapolated back to the laser source. The measured wavelength of the diffuse photon density wave in the homogeneous Intralipid was ~18 cm.

In Fig. 1(c) we exhibit the constant amplitude contours of the wave at 830 nm, and thus demonstrate the diffuse photon density wave character of the reradiated waves. We see clearly that *the reradiated wave originates from within the absorbing obstacle.* From the contours we deduce a source origin of ~4.6 cm. The overall quantum efficiency of the dye from 780 to 830 nm was $\sim10^{-5}$. Similar conclusions could be drawn from the phase contours although the phase data were more sensitive to the small light leakages at 780 nm and were therefore considerably noisier. The diffuse photon density wavelength at 830 nm was measured to be ~27 cm, somewhat larger than the wave at 780 nm reflecting the larger light diffusion constant for 830 nm light in Intralipid. We have also compared reradiated waves from spherical and cylindrical objects. The measurements clearly show that the contours in the case of the cylinder are more elliptical than those of the sphere, thereby demonstrating that the reradiation technique can be sensitive to the shape of the obstacle.

Our scattering experiments fall into two categories. We consider the pure absorptive spheres first (see Fig. 2). We have measured constant phase and amplitude contours for diffuse density waves traveling in different concentrations of Intralipid and then scattering from a 4.0-cm-diam absorptive sphere. The sphere was saturated with ink so that the fraction of incident light at 816 nm transmitted through the sphere was below our detection limit of $\sim10^{-6}$. Nevertheless, we detect robust wave fronts on the other side of the sphere. These wave fronts are formed by the diffraction of the wave around the sphere.

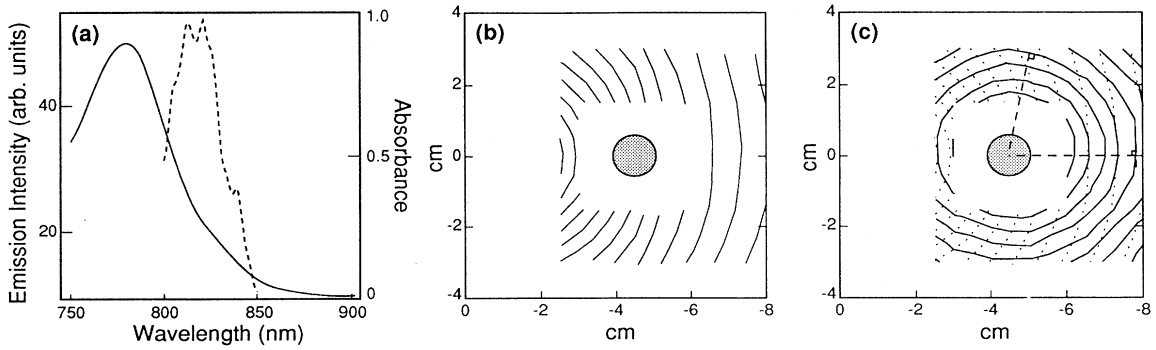

FIG. 1. (a) Indocyanine green absorption (solid line) and emission (dashed line) spectra. The laser radiates at 780 nm. (b) Constant amplitude contours of the incident diffuse photon density wave at 780 nm. (c) Constant amplitude contours at 830 nm (solid lines) clearly exhibiting the reradiated nature of the wave. The dashed lines are the amplitude contours at 780 nm, and the center of the radiator is located by finding the intersection of the lines normal to these contours. The amplitude of the adjacent contours decreases by a factor of 0.3.

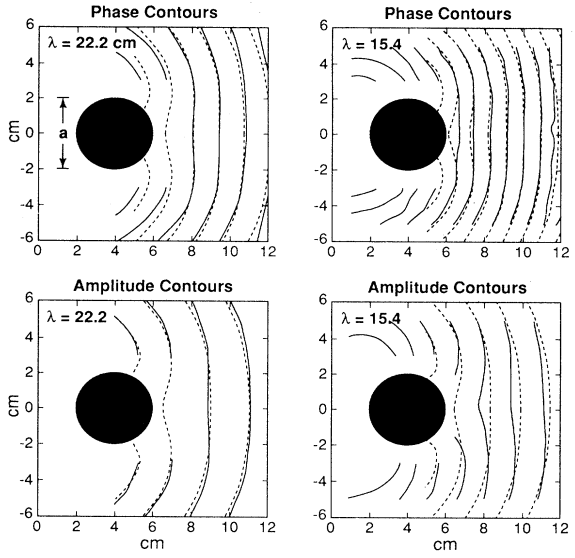

FIG. 2. These plots show the diffraction of a diffuse photon density wave by a spherical absorber ($a=4.0$ cm). The light source is at the origin and generates a wave with a wavelength of 22.2 cm in the plots on the left, and a wavelength of 15.4 cm in the plots on the right. Our experimental (theoretical) results are the solid (dashed) curves. The phase contours are plotted every 20° and the amplitude contours are plotted in decreasing intervals of e^{-1}.

We have modeled this effect in a simple way. We replaced the sphere by a totally absorbing disk of the same diameter. The disk was chosen to lie in a plane containing the center of the sphere, with surface normal pointing in the z direction. Then we calculated the diffraction from this disk using the standard Kirchoff construction [10] that, as we have discussed previously [5], should apply to these waves, i.e.,

$$U(x_p,y_p=0,z_p)=\frac{kz_p}{2\pi i}\int_s U(\mathbf{R}_1)\frac{e^{ikR_2}}{R_2^2}\left[\frac{i}{kR_2}+1\right]dx\,dy\ . \tag{1}$$

The construction is depicted in Fig. 3(a). Here $U(\mathbf{R}_1)$ is the complex amplitude of the light energy density in the plane of the disk, R_1 is the length of the vector from the source at position $\mathbf{R}_s=(x_s=0,\ y_s=0,\ z_s)$ to a point $\mathbf{A}=(x,y,z=0)$ on the diffraction plane, and R_2 is the length of the vector going from $\mathbf{A}$ to the detection point $\mathbf{R}_p=(x_p,y_p=0,z_p)$. The Green's function is derived from the point source solution for diffuse photon density waves in an infinite homogeneous medium [11] so that k is complex.

Our experimental (theoretical) results are the solid (dotted) curves in Fig. 2. We see that our simple model approximates the measured wave-front distortion reasonably well. We note that there are no free parameters in our fit, and that it was important to incorporate the effects of absorptive loss in the Intralipid in order to obtain the best agreement. The model appears to fit the experimental results better for bigger ratios of diffuse photon density wavelength to object diameter. Of course,

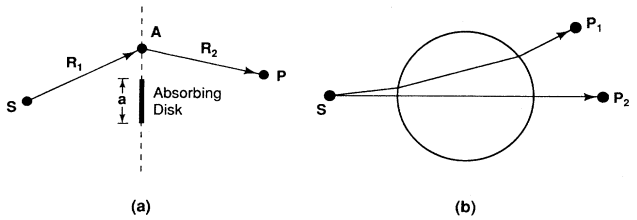

FIG. 3. (a) In our diffraction model the sphere is replaced by an absorbing disk of the same diameter ($a=4.0$ cm), which lies in a plane through the center of the sphere. R_1 is the distance from the source S to a point $\mathbf{A}$ in the diffraction plane (dashed line) and R_2 is the distance from $\mathbf{A}$ to the image point P. Here we take the z axis to be normal to the diffraction plane, and we let the diffraction plane coincide with the xy plane (i.e., $z=0$). The wave front at P is calculated by integrating the standard Kirchoff equation over the diffraction plane [11]. (b) In the ray model the wave front is calculated by determining the phase and amplitude of rays, which are refracted through a spherical lens.

our function $U(\mathbf{R}_1)$ in the plane of the disk is only approximately correct as a result of shadowing and diffraction by the front portion of the sphere. A similar effect will modify the scattered wave. Nevertheless, the model captures the qualitative physics of the scattering.

In Fig. 4 we show the constant phase contours (solid line) arising from the scattering of a *nonabsorptive* sphere. The Intralipid surrounding the sphere had the same concentration in both experiments, but the concentration of Intralipid inside the sphere was either smaller [Fig. 4(a)] or larger [Fig. 4(b)] than the surrounding medium. We observe that the patterns are different. Results of our simple modeling of these effects are described below.

One model is derived from ray optics where we simply treated the scatterer like a spherical lens with a different diffusional index of refraction than the surrounding medium. The basic idea of the model is depicted in Fig. 3(b).

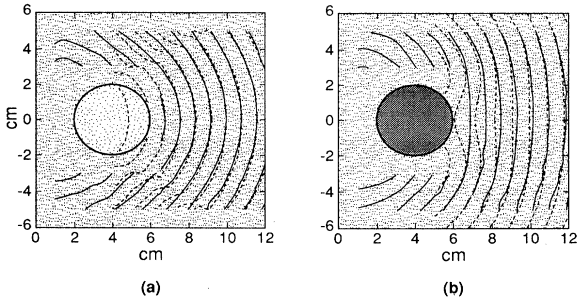

FIG. 4. The scattering of a diffuse photon density waves by purely dispersive spheres. (a) The Intralipid concentration within the spherical shell is 0.125%, less than the surrounding medium. (b) The Intralipid concentration is 2.8%, greater than the surrounding medium. For both, the surrounding Intralipid is the same, the source is located at the origin, and the sphere has a diameter of 4.0 cm and is centered at $x=4.0$ cm, $y=0.0$ cm. The phase contours are drawn every 20° for our experimental (solid lines) and theoretical (dashed lines) results. The theoretical results were calculated in (a) by the ray model and in (b) by the diffraction model.

To get the complex wave amplitude we simply kept track of the amplitude and phase for points along the rays emerging from the source. Some of the rays were refracted through the sphere, others were not. This model ignores multiple scattering in the sphere, since the waves are heavily damped.

Again, we do not expect the model to give perfect quantitative agreement with the measurements since diffraction effects are omitted. However, because the rays transmitted through the sphere will have a larger amplitude than pathways around the sphere, we might expect that the ray picture would work well when the diffusional index of refraction of the sphere is less than that of the surrounding Intralipid. This behavior was observed [see Fig. 4(a)]. For near axis rays the model also predicts an apparent source position at $z_s = 3.5$ cm. This is easily verified by standard ray construction techniques.

The ray method did not work well for dense spheres. The dense sphere acts more like an absorber, since the diffuse photon density wave will be significantly attenuated upon traveling through the sphere. For this reason one might expect the purely diffractive model discussed earlier to work better. Indeed, this is what was observed [see Fig. 4(b)].

In the experiments we have described, spatial inhomogeneities of varying nature were detected using diffuse photon density waves. The incident wave fronts were shown to diffract around and refract through objects, and by a clever use of an absorptive dye, new wave fronts were created within the medium by objects that reradiate at different *optical* wavelengths. Practical biomedical imaging systems with diffusing light will take advantage of these types of distortions in order to detect inhomogeneities. The reradiation technique can be applied, since emissive dyes (i.e., contrast agents) are known to be preferentially accumulated at spatial inhomogeneities [12], such as breast tumors and infarcted regions of brain tissue. In this case, the presence of any reradiated wave would signal the existence of the tumor or infarcted region, and the location of its center is reconstructed using the shape of the reradiated wave fronts. We are presently implementing this idea along with delineated antenna arrays of diffuse photon density waves to improve detection capabilities [13]. The diffracted wave fronts can also be used to detect tumors, with or without the use of absorbing dyes. Here the improved sensitivity is achieved through the interference of phased arrays of diffuse light sources [7,13].

We acknowledge useful conversations with Peter Kaplan, Tom Lubensky, K. S. Reddy, and Jack Leigh. A.G.Y. gratefully acknowledges partial support from the National Science Foundation through the Presidential Young Investigator program and Grant No. DMR-9003687, and from the Alfred P. Sloan Foundation. B.C. gratefully acknowledges support from HL-44125, ACSBE-B, NS-27346, NIM Inc., and Hamamatsu Photonics.

[1] A. Ishimaru, *Wave Propagation and Scattering in Random Media* (Academic, New York, 1978), Vol. 1.

[2] E. Gratton, W. Mantulin, M. J. van de Ven, J. Fishkin, M. Maris, and B. Chance, in *Proceedings of the Third International Conference: Peace through Mind/Brain Science,* Hamamatsu, Japan, 1990 (Hamamatsu Photonics, Hamamatsu, 1990), p. 183.

[3] J. M. Schmitt, A. Knuttel, and J. R. Knudsen, J. Opt. Soc. Am. A **9**, 1832 (1992).

[4] J. Fishkin and E. Gratton J. Opt. Soc. Am. A **10**, 127 (1993).

[5] M. A. O'Leary, D. A. Boas, B. Chance, and A. G. Yodh, Phys. Rev. Lett. **69**, 2658 (1992).

[6] See also, for example, B. J. Tromberg, L. O. Svaasand, T. Tsay, R. C. Haskell, and M. W. Berns, in *Proceedings of the SPIE '91 Vol. 1525, Future Trends in Biomedical Applications of Lasers,* Berlin, 1991, edited by S. Jaques (International Society for Optical Engineering, Bellingham, 1991), p. 52, and references therein.

[7] B. Chance, K. Kang, L. He, and J. Weng, in *Proceedings of the International Society on Oxygen Transport to Tissue (ISOTT),* Mainz, Germany, 1992, edited by P. Baupel (Plenum, New York, 1993).

[8] The Intralipid used here can be obtained from Kabi Pharmacia in Clayton, NC.

[9] Indocyanine-green is a water soluable, tricarbocyanine dye. We obtained the dye from Hynson, Wescott & Dunning, Inc., Baltimore, MD 21201.

[10] J. D. Jackson, *Classical Electrodynamics* (Wiley, New York, 1975), Chap. 9.

[11] The Green's function for this problem is derived from a superposition of Green's-function solutions of the Helmholtz equation (i.e., of the form $e^{ikr}/4\pi r$). We chose a superposition to satisfy Dirichlet boundary conditions on our diffraction plane at $z=0$. Therefore, (1) is derived from the integral $\int U(\mathbf{R}_1)(dG_D/dz)dx\,dy$ over the diffraction plane, with $G_D(R,R')=[e^{ikR}/R - e^{ikR'}/R']/4\pi$, where $\mathbf{R}=\mathbf{R}_p-\mathbf{A}$, $\mathbf{R}'=\mathbf{R}_{p'}-\mathbf{A}$, and $\mathbf{R}_{p'}$ is just the image of $\mathbf{R}_p$ reflected about the diffraction plane.

[12] F. W. Flickinger, J. D. Allison, R. Sherry, and J. C. Wright, in *Proceedings of the Society of Magnetic Resonance in Medicine 11th Annual Scientific Meeting,* Berlin, Germany, 1992 (Society of Magnetic Resonance in Medicine, San Francisco, 1992); R. N. Bryan, *ibid.*

[13] M. A. O'Leary, D. A. Boas, B. Chance, and A. G. Yodh, in *SPIE Proceedings of the Biomedical Optics Society,* Los Angeles, 1993, edited by B. Chance and R. Alfano (International Society for Optical Engineering, Bellingham, 1993).